

# RARE $B$ DECAYS AT BELLE AND BABAR

Hiroaki Aihara\*

Department of Physics

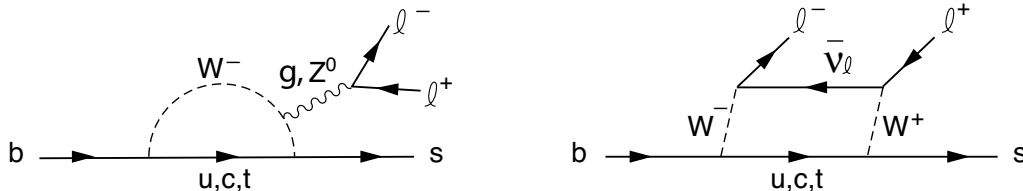
University of Tokyo, Tokyo 113-0033, Japan

## ABSTRACT

Results from two asymmetric-energy  $e^+e^-$  collider experiments, Belle at KEK and BaBar at SLAC, have been presented with an emphasis on rare  $B$  decays. A search for a rare  $\tau$  decay,  $\tau \rightarrow \mu\gamma$ , by Belle has also been shown.

---

\*Supported in part by a Grant-in-Aide for Scientific Research on Priority Areas (Origin of Mass and Super Symmetry) from the Ministry of Education, Culture, Sports, Science and Technology.

Figure 1: Schematic diagram of  $b \rightarrow s\ell^+\ell^-$  decay.

## 1 Introduction

Asymmetric-energy  $e^+e^-$  colliders at  $\Upsilon(4S)$  have shown excellent performance in delivering high luminosity. As of July 1st 2003, Belle at KEKB and BaBar at PEP-II have accumulated  $158.7 \text{ fb}^{-1}$  and  $130.7 \text{ fb}^{-1}$ , respectively. With this impressive amount of data,  $B$ -factory experiments have become a new searching ground for rare processes which may lead to new physics.

In particular, the flavor-changing neutral current (FCNC) decays  $b \rightarrow s\ell^+\ell^-$  ( $\ell = e, \mu$ ) and  $b \rightarrow s\gamma$  are of great interest. FCNC decays are forbidden at tree level in the Standard Model (SM); they proceed only at a low rate via higher-order loop diagrams. Their total branching fractions are very sensitive to physics beyond the SM as it may be affected by the presence of charged Higgs or SUSY particles in the loop.<sup>1</sup> Electroweak FCNC decay  $b \rightarrow s\ell^+\ell^-$  is suppressed over radiative  $b \rightarrow s\gamma$  by an additional  $\alpha_{em}$  factor, as shown in Fig. 1, resulting in  $Br(b \rightarrow s\ell^+\ell^-) \sim 10^{-6}$ . Thus, observation of this very rare decay had eluded us before Belle and BaBar.

Similarly, the lepton-flavor-violating decay  $\tau \rightarrow \mu\gamma$  is of interest. It is strictly forbidden within SM. However, some supersymmetric models, left-right symmetric models, and others<sup>2</sup> predict a branching fraction in the range of  $10^{-7} - 10^{-9}$ , which is accessible at an  $e^+e^-$   $B$ -factory. The branching fraction of  $\tau \rightarrow \mu\gamma$  could be enhanced by a factor of  $10^5 - 10^6$  over that of  $\mu \rightarrow e\gamma$ , because relevant kinematic factors depend on powers of  $m_\tau/m_\mu$ . This process has previously been searched for by MARK-II,<sup>3</sup> ARGUS,<sup>4</sup> DELPHI,<sup>5</sup> CLEO,<sup>6</sup> and BaBar.<sup>7</sup> The most sensitive upper limit, reported by CLEO using  $13.8 \text{ fb}^{-1}$ , is  $Br(\tau \rightarrow \mu\gamma) < 1.1 \times 10^{-6}$  at 90% confidence level.

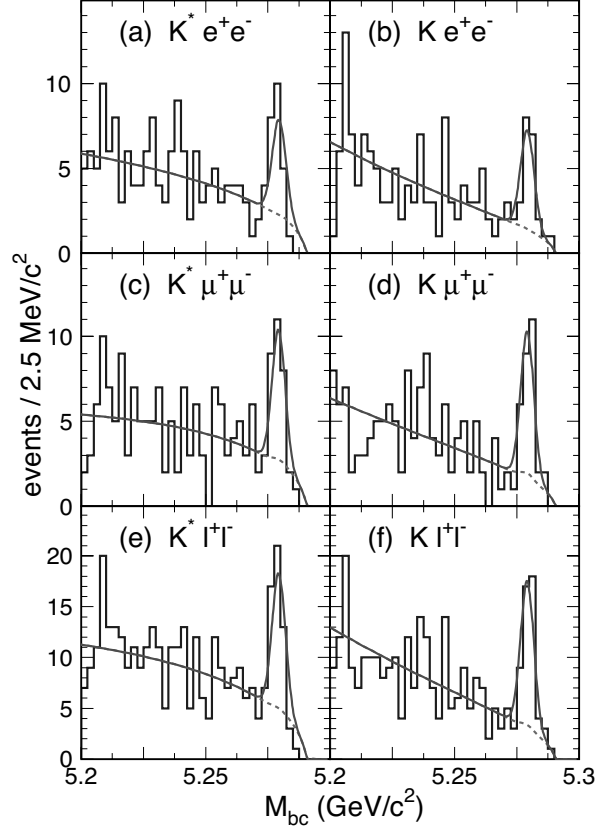


Figure 2: Belle observation of  $B \rightarrow K^* \ell^+ \ell^-$  and  $K \ell^+ \ell^-$ .  $M_{bc}$  distributions for  $K^* \ell^+ \ell^-$  and  $K \ell^+ \ell^-$  samples are shown. Solid and dotted curves show the results of the fits and the background contributions, respectively.

## 2 Electroweak Rare $B$ Decays

### 2.1 Exclusive $B \rightarrow K^{(*)} \ell^+ \ell^-$ measurement

Belle reported the first observation of exclusive  $B \rightarrow K \ell^+ \ell^-$  decay<sup>8</sup> and inclusive  $B \rightarrow X_s \ell^+ \ell^-$ .<sup>9</sup> Belle has updated the analysis of exclusive measurement based on a  $140 \text{ fb}^{-1}$ .<sup>10</sup> This new analysis includes the measurement of  $B \rightarrow K^* \ell^+ \ell^-$ .

The  $b \rightarrow s \ell^+ \ell^-$  decay candidates are selected based on its clear signature, a high momentum lepton pair. The  $B \rightarrow K^{(*)} \ell^+ \ell^-$  signal is isolated using the beam-energy constrained mass  $M_{bc} = \sqrt{E_{\text{beam}}^{*2} - p_B^{*2}}$  and the energy difference  $\Delta E = E_B^* - E_{\text{beam}}^*$ , where  $E_{\text{beam}}^*$  is the beam energy and  $E_B^*$  and  $p_B^*$  are the measured energy and momentum of the  $B$  candidate, all measured in the  $\Upsilon(4S)$  rest frame. For  $B^0 \rightarrow K^{*0} \ell^+ \ell^-$  decay,  $K^{*0} \rightarrow K^+ \pi^-$  decay is used, while

Table 1:  $B \rightarrow K^{(*)}\ell^+\ell^-$  branching fractions.

Mode	Belle (140 fb <sup>-1</sup> ) [ $\times 10^{-7}$ ]	BaBar (113 fb <sup>-1</sup> ) [ $\times 10^{-7}$ ]	SM prediction <sup>12</sup> [ $\times 10^{-7}$ ]
$B \rightarrow Ke^+e^-$	$4.8_{-1.3}^{+1.5} \pm 0.3 \pm 0.1$	$7.9_{-1.7}^{+1.9} \pm 0.7$	
$B \rightarrow K\mu^+\mu^-$	$4.8_{-1.1}^{+1.3} \pm 0.3 \pm 0.2$	$4.8_{-2.0}^{+2.5} \pm 0.4$	
$B \rightarrow K\ell^+\ell^-$	$4.8_{-0.9}^{+1.0} \pm 0.3 \pm 0.1$	$6.9_{-1.3}^{+1.5} \pm 0.6$	$3.5 \pm 1.2$
$B \rightarrow K^*e^+e^-$	$14.9_{-4.6-1.3}^{+5.2+1.1} \pm 0.3$	$10.0_{-4.2}^{+5.0} \pm 1.3$	
$B \rightarrow K^*\mu^+\mu^-$	$11.7_{-3.1}^{+3.6} \pm 0.8 \pm 0.6$	$12.8_{-6.2}^{+7.8} \pm 1.7$	
$B \rightarrow K^*\ell^+\ell^-$	$11.5_{-2.4}^{+2.6} \pm 0.7 \pm 0.4$	$8.9_{-2.9}^{+3.4} \pm 1.1$	$11.9 \pm 3.9$

$K^{*+} \rightarrow K_S^0\pi^+$  and  $K^+\pi^0$  decays are used for  $B^+ \rightarrow K^{*+}\ell^+\ell^-$  decay. The signal windows are defined as  $|M_{bc} - M_B| < 0.007 \text{ GeV}/c^2$  for both lepton modes and  $-0.055(-0.035) \text{ GeV} < \Delta E < 0.035 \text{ GeV}$  for the electron (muon) mode. Figure 2 shows  $M_{bc}$  distributions for  $K^*\ell^+\ell^-$  and  $K\ell^+\ell^-$  samples. Solid and dotted curves show the results of the fits and the background contributions, respectively. Belle observes  $37.9_{-6.9}^{+7.6}(\text{stat})_{-1.1}^{+1.0}(\text{syst})$   $K \rightarrow \ell^+\ell^-$  signal events with a significance of 7.4, and, for the first time,  $35.8_{-7.3}^{+8.0}(\text{stat}) \pm 1.7(\text{syst})$   $K^*\ell^+\ell^-$  signal events with a significance of 5.7.

BaBar has obtained the results based on a 113 fb<sup>-1</sup> data sample.<sup>11</sup> A clear signal for  $B \rightarrow K\ell^+\ell^-$  is observed with a significance greater than 8 as shown in Fig. 3. Figure 4 shows evidence, found by BaBar, for  $B \rightarrow K^*\ell^+\ell^-$  signal with a significance of 3.3.

Table 1 summarizes the measured branching fractions. For the combined  $B \rightarrow K^*\ell^+\ell^-$  results,  $Br(B \rightarrow K^*\ell^+\ell^-) = Br(B \rightarrow K^*\mu^+\mu^-) = 0.75 \times Br(B \rightarrow K^*e^+e^-)$  is assumed which compensates the enhancement at the  $q^2 = 0$  pole that appears more significantly in  $K^*e^+e^-$ , using the expected SM ratio.<sup>12</sup> The measured branching fractions agree with the SM predictions of  $(3.5 \pm 1.2) \times 10^{-7}$  for  $B \rightarrow K\ell^+\ell^-$  and  $(11.9 \pm 3.9) \times 10^{-7}$  for  $B \rightarrow K^*\ell^+\ell^-$ , taken from Ref.<sup>12</sup> The experimental errors are already much smaller than the uncertainties in the SM predictions and the variations due to different model-dependent assumptions used to account for the hadronic uncertainties.

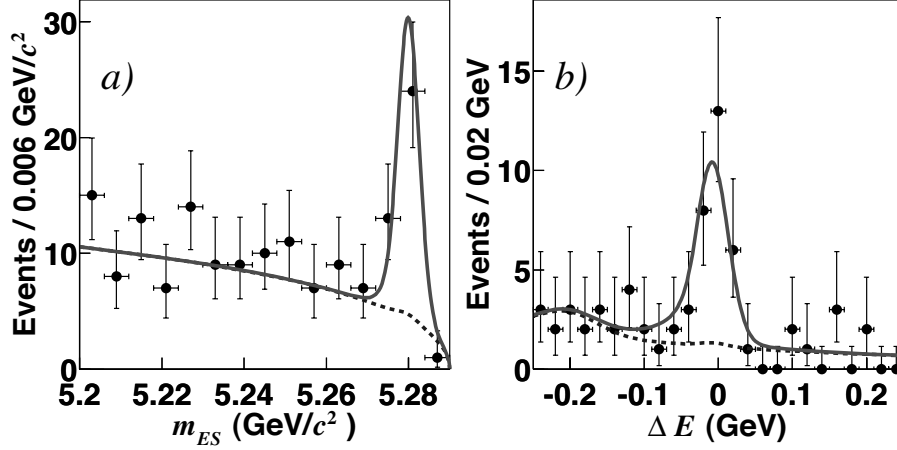


Figure 3: BaBar observation of  $B \rightarrow K\ell^+\ell^-$ . (a)  $m_{ES}(=m_{bc})$  distribution after requiring  $-0.11 < \Delta E < 0.05 \text{ GeV}$  and (b)  $\Delta E$  distribution after requiring  $|m_{ES} - m_B| < 6.6 \text{ MeV}/c^2$  ( $2.6\sigma$ ). The solid curve is the sum of all fit components, including signal; the dashed curve is the sum of all background components.

## 2.2 Inclusive $B \rightarrow X_s\ell^+\ell^-$ measurement

Belle has measured the inclusive  $B \rightarrow X_s\ell^+\ell^-$  branching fraction<sup>9</sup> from a  $60 \text{ fb}^{-1}$  data sample by reconstructing the  $X_s$  final state with one kaon ( $K^+$  or  $K_S^0$ ) and up to four pions, of which one pion is allowed to be  $\pi^0$ . Assuming the  $K_L^0$  contribution is the same as  $K_S^0$ , this set of final states covers  $82 \pm 2\%$  of the signal. In addition,  $M(X_s)$  is required to be below  $2.1 \text{ GeV}/c^2$  in order to reduce backgrounds. For leptons, minimum momentum of  $0.5 \text{ GeV}/c$  for electrons,  $1.0 \text{ GeV}/c$  for muons and  $M(\ell^+\ell^-) > 0.2 \text{ GeV}/c^2$  are required.

A new result is reported by BaBar with a  $78 \text{ fb}^{-1}$  data sample based on a similar method.<sup>13</sup> BaBar includes only up to two pions in  $X_S$ , corresponding to 75% of the signal, and require  $M(X_S) < 1.8 \text{ GeV}/c^2$ . The minimum muon momentum of  $0.8 \text{ GeV}/c$  is lower than that for Belle analysis.

The signal of  $60 \pm 14$  events from Belle with a statistical significance of 5.4 is shown in Fig. 5, and  $41 \pm 10$  events from BaBar with a significance of 4.6 is shown in Fig. 6. Resulting branching fractions are consistent with each other as given in Table 2. The average value is

$$Br(B \rightarrow X_s\ell^+\ell^-) = (6.2 \pm 1.1^{+1.6}_{-1.3}) \times 10^{-6}.$$

The branching fraction results are for the dilepton mass range above  $M(\ell^+\ell^-) >$

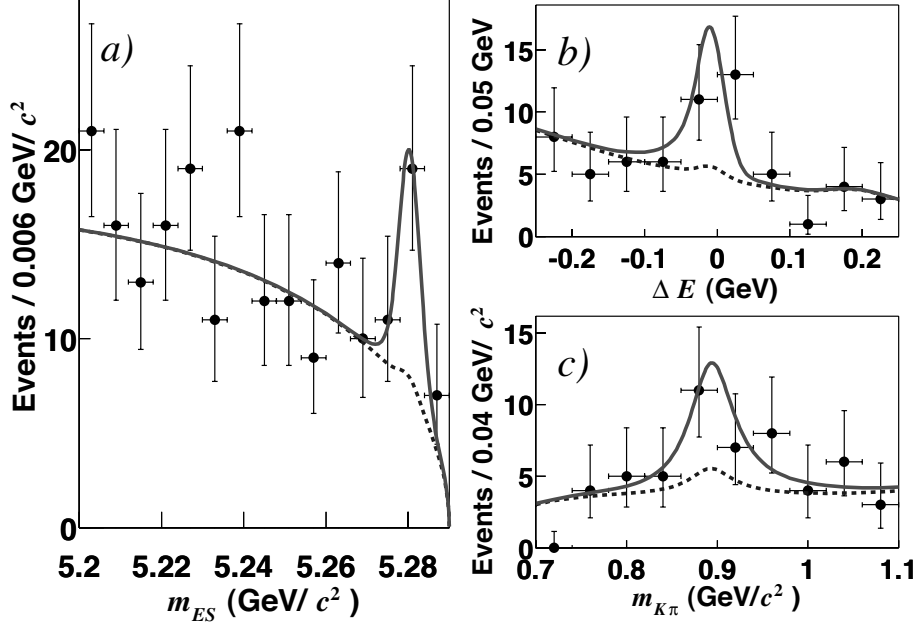


Figure 4: Evidence for  $B \rightarrow K^* \ell^+ \ell^-$  found by BaBar. (a)  $m_{ES}(= m_{bc})$  distribution after requiring  $-0.11 < \Delta E < 0.05$  GeV and  $0.817 < m_{K\pi} < 0.967$  GeV/c<sup>2</sup>, and (b)  $\Delta E$  distribution after requiring  $|m_{ES} - m_B| < 6.6$  MeV/c<sup>2</sup> ( $2.6\sigma$ ) and  $0.817 < m_{K\pi} < 0.967$  GeV/c<sup>2</sup>, and (c)  $m_{K\pi}$  after requiring  $|m_{ES} - m_B| < 6.6$  MeV/c<sup>2</sup> and  $-0.11 < \Delta E < 0.05$  GeV. The solid curve is the sum of all fit components, including signal; the dashed curve is the sum of all background components.

0.2 GeV/c<sup>2</sup> and are interpolated in the  $J/\psi$  and  $\psi'$  regions that are removed from the analysis, assuming no interference with these charmonium states. The results may be compared with the SM prediction<sup>12</sup> of  $(4.2 \pm 0.7) \times 10^{-6}$  integrated over the same dilepton mass range of  $M(\ell^+ \ell^-) > 0.2$  GeV/c<sup>2</sup>. With this requirement, the effect of the  $q^2 = 0$  pole becomes insignificant, giving almost equal branching fractions for the electron and muon modes. The measured branching fractions agree with the SM prediction within experimental error. The systematic error is dominated by the uncertainty in the  $M(X_S)$  distribution due to uncertainty of the fraction of  $B \rightarrow K^{(*)} \ell^+ \ell^-$  components. We expect this uncertainty will be significantly reduced as the precision of exclusive measurements improves. Distributions for  $M(X_S)$  and  $M(\ell^+ \ell^-)$  are shown in Figs. 7 and 8, and are again consistent with the SM predictions.

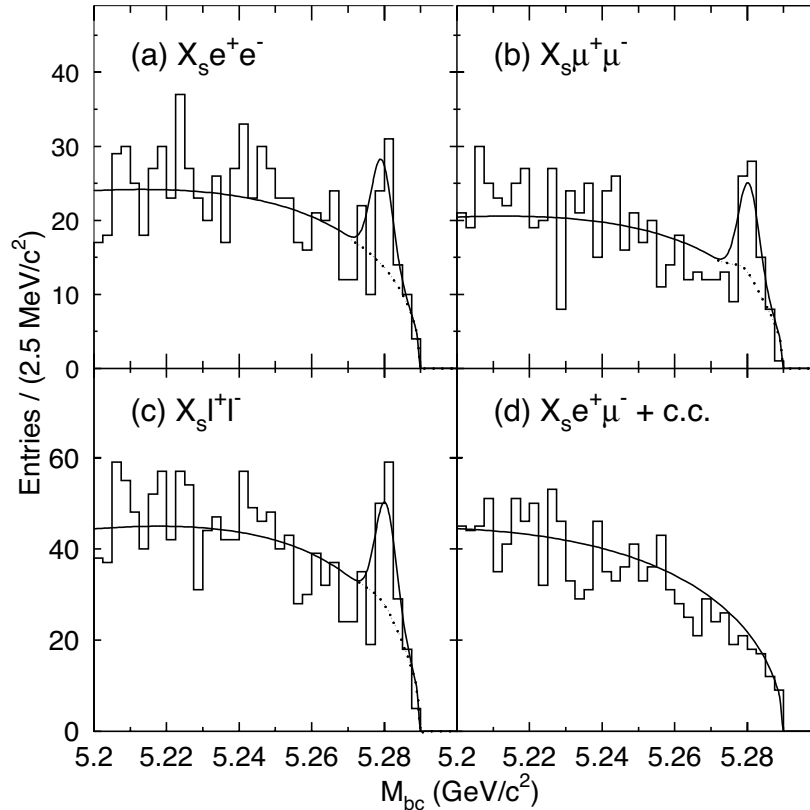


Figure 5:  $B \rightarrow X_s \ell^+ \ell^-$  signal measured from Belle. The  $X_s e^+ \mu^-$  sample represents the combinatorial backgrounds.

### 3 Search for Rare $\tau$ Decays

Belle has searched for the  $\tau \rightarrow \mu\gamma$  decay based on an  $86.3 \text{ fb}^{-1}$  data sample.<sup>14</sup> The analysis is to search for an event consisting of exactly two oppositely-charged tracks and at least one photon candidate, which is consistent with a  $\tau^+ \tau^-$  event in which one  $\tau$  decays to  $\mu\gamma$  and the other  $\tau$  decays to a non-muon charged particle, neutrino(s) and any number of  $\gamma$ s. The dominant sources of background are  $e^+ e^- \rightarrow \mu^+ \mu^- \gamma$  and  $\tau^+ \tau^- \gamma$ , in which the photon is radiated from the initial state.

The charged track that forms a  $\tau \rightarrow \mu\gamma$  candidate is required to have  $p > 1.0 \text{ GeV}/c$  and to be identified as a muon based on the difference between the range calculated from the particle momentum and that measured by a muon detector. The other track (on the “tag-side”) is required not to be a muon to reduce  $e^+ e^- \rightarrow \mu^+ \mu^- \gamma$  background. Photon candidates are required to be within

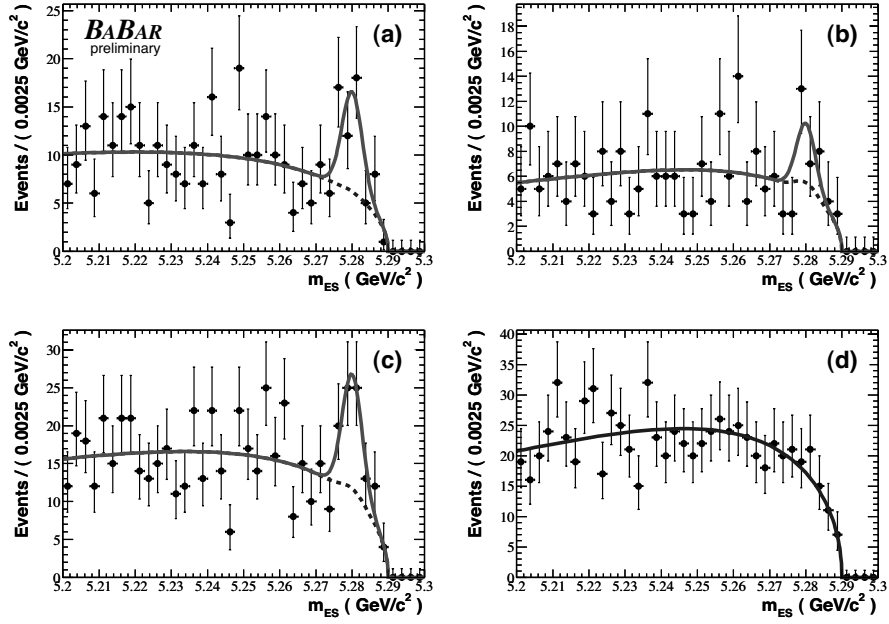


Figure 6: (a)  $B \rightarrow X_s e^+ e^-$ , (b)  $B \rightarrow X_s \mu^+ \mu^-$ , (c)  $B \rightarrow X_s \ell^+ \ell^-$  signals with the (d)  $X_s e^+ \mu^-$  sample from BaBar.

the barrel calorimeter. The photon that forms a  $\tau \rightarrow \mu\gamma$  candidate is required to have an energy  $E_\gamma > 0.5$  GeV in order to avoid a spurious combination of a low-energy  $\gamma$  with the muon.

To reject Bhabha scattering and  $\mu^+ \mu^-$  production, the sum of the energies of the two charged tracks and the photon composing the  $\mu\gamma$  is required to be less than 9.0 GeV in the  $\Upsilon(4S)$  rest frame (CMS). A restriction of the opening angle (measured in CMS) between the  $\mu$  and  $\gamma$ ,  $0.4 < \cos \theta_{\mu\gamma}^* < 0.8$ , is particularly powerful to reject background events arising mostly from  $e^+ e^- \rightarrow \tau^+ \tau^-$ ,  $\tau \rightarrow \pi^0 X$ .

Table 2:  $B \rightarrow X_s \ell^+ \ell^-$  branching fractions.

Mode	Belle (60 fb <sup>-1</sup> ) [ $\times 10^{-6}$ ]	BaBar (78 fb <sup>-1</sup> ) [ $\times 10^{-6}$ ]	SM prediction <sup>12</sup> [ $\times 10^{-6}$ ]
$B \rightarrow X_s e^+ e^-$	$5.0 \pm 2.3^{+1.3}_{-1.1}$	$6.6 \pm 1.9^{+1.9}_{-1.6}$	
$B \rightarrow X_s \mu^+ \mu^-$	$7.9 \pm 2.1^{+2.1}_{-1.5}$	$5.7 \pm 2.8^{+1.7}_{-1.4}$	
$B \rightarrow X_s \ell^+ \ell^-$	$6.1 \pm 1.4^{+1.4}_{-1.1}$	$6.3 \pm 1.6^{+1.8}_{-1.5}$	$4.2 \pm 0.7$



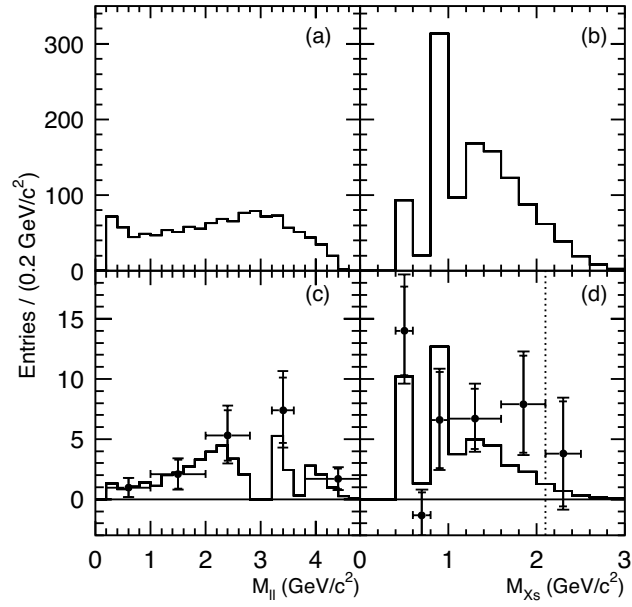


Figure 7:  $M(\ell^+\ell^-)$  (left) and  $M(X_S)$  (right) distributions for  $B \rightarrow X_s \ell^+ \ell^-$  from Belle (points with error bars), compared with the SM predictions before (top) and after (bottom) including detector acceptance effects.

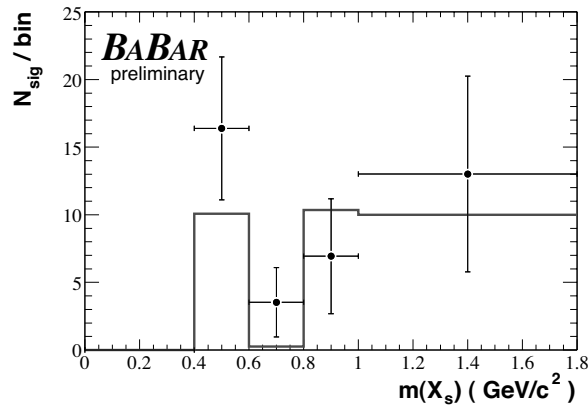


Figure 8:  $M(X_S)$  distribution for  $B \rightarrow X_s \ell^+ \ell^-$  from BaBar.

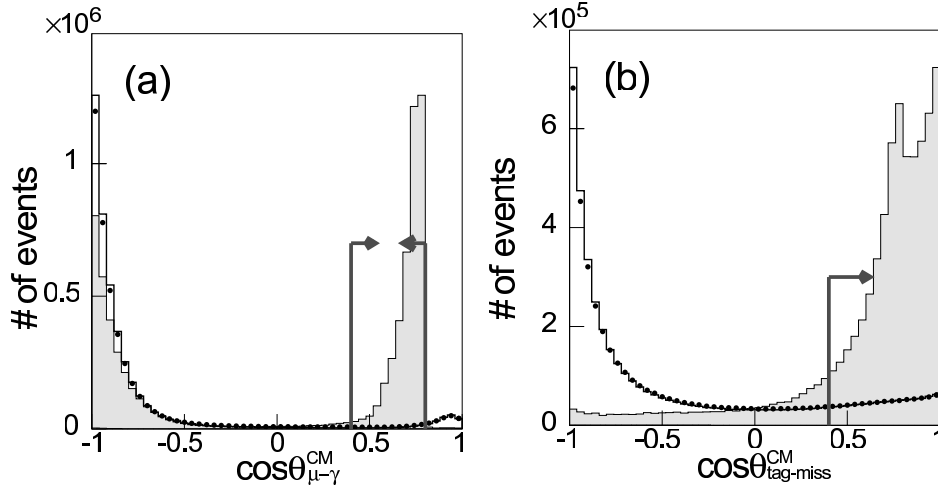


Figure 9: Belle  $\tau \rightarrow \mu\gamma$  search. Distributions of the opening angle between (a) the  $\mu$  and  $\gamma$  on the signal side, and (b) the track on the other side and the missing momentum. MC distributions for signal and  $\tau^+\tau^-$  events are indicated by shaded and open histograms, respectively, and data by closed circles. The arrows show the selected ranges.

This process forms the backward peak in the open histogram in Fig. 9(a). The opening angle between two tracks is required to be greater than  $90^\circ$ .

In order to require presence of a neutrino in the event,  $\vec{p}_{\text{miss}}$  is defined as the residual momentum vector calculated by subtracting the vector sum of all visible momenta (both from tracks and photon candidates) from the sum of the  $e^+$  and  $e^-$  beam momenta. Constraints on the momentum and polar angle of the missing particle(s),  $p_{\text{miss}} > 0.4 \text{ GeV}/c$  and  $-0.866 < \cos\theta_{\text{miss}} < 0.956$ , respectively, are imposed to increase the probability that the missing particle(s) is an undetected neutrino(s) rather than  $\gamma$ s or charged particles falling outside the acceptance of the detector. To remove  $\tau^+\tau^-$  events, a requirement to the opening angle between the tagging track and the missing particle,  $\cos\theta_{\text{tag-miss}}^* > 0.4$ , is applied as shown in Fig. 9(b).

Furthermore, a condition is imposed on the relation between  $p_{\text{miss}}$  and the mass-squared of a missing particle ( $m_{\text{miss}}^2$ ). The latter is defined as  $E_{\text{miss}}^2 - p_{\text{miss}}^2$ , where  $E_{\text{miss}}$  is 11.5 GeV (the sum of the beam energies) minus the sum of all visible energy and is calculated assuming the muon(pion) mass for the charged track on the signal (tag) side. The requirement of  $p_{\text{miss}} > -5 \times m_{\text{miss}}^2 - 1$  and

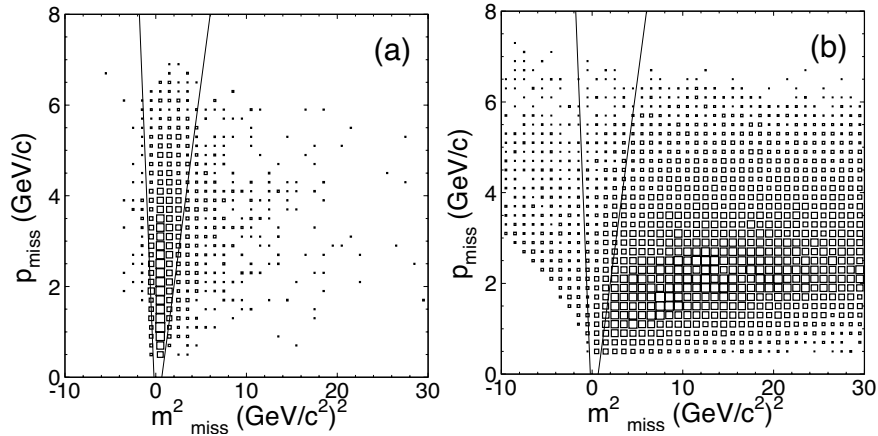


Figure 10: Belle  $\tau \rightarrow \mu\gamma$  search.  $p_{\text{miss}}$  vs  $m_{\text{miss}}^2$  distribution. The selection boundary is indicated by two lines for (a) signal MC events and (b)  $\tau^+\tau^-$  MC events.

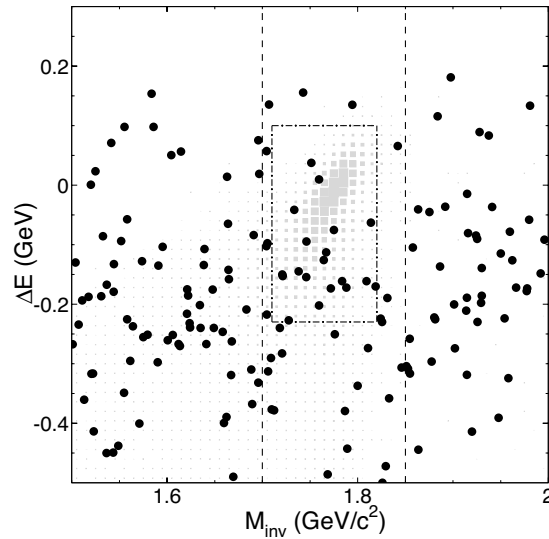


Figure 11: Belle  $\tau \rightarrow \mu\gamma$  search. Remaining events in data (circles) and the expected density for signal MC (shaded) in the  $\Delta E$  vs  $M_{\text{inv}}$  plane. The region between the dashed lines is kept excluded until the selection criteria are finalized and the expected background estimated. The signal box is indicated by a dash-dotted box.

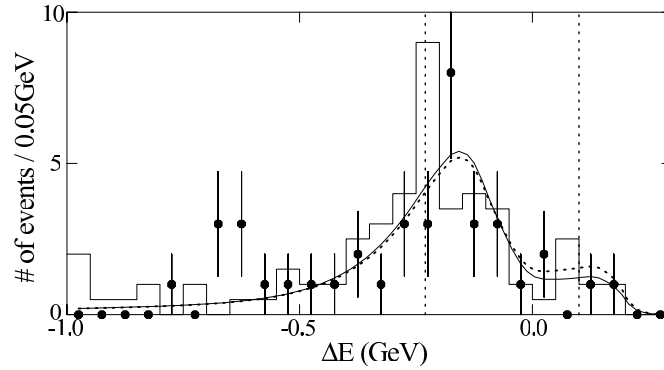


Figure 12: Belle  $\tau \rightarrow \mu\gamma$  search.  $\Delta E$  distribution in the signal region,  $1.71 < M_{\text{inv}} < 1.82 \text{ GeV}/c^2$ . The data are points with error bars. The expected background from MC simulations is indicated by curves and an average of both sidebands is shown by the histogram.

$p_{\text{miss}} > 1.5 \times m_{\text{miss}}^2 - 1$ , where  $p_{\text{miss}}$  is in  $\text{GeV}/c$  and  $m_{\text{miss}}$  is in  $\text{GeV}/c^2$ , removes 98% of the remaining  $\tau^+\tau^-$  background (see Fig. 10) and 86% of the  $\mu^+\mu^-$  background.

After these selection requirements, 713 events remain in the data without any restriction on the mass and momentum of the  $\mu\gamma$  system. The detection efficiency is evaluated by a Monte Carlo simulation to be  $\epsilon = 12.0 \pm 0.1\%$ . The candidate  $\mu\gamma$  system should have an invariant mass ( $M_{\text{inv}}$ ) close to the  $\tau$  mass and an energy close to the beam energy in the cms,  $\Delta E = E_{\mu\gamma}^* - E_{\text{beam}}^* \sim 0$ . The resulting  $\Delta E$  vs  $M_{\text{inv}}$  distribution is shown in Fig. 11. Because of the photon's energy leakage from the calorimeter and initial-state radiation, the MC simulation exhibits a long low-energy tail across the  $\Delta E$  vs  $M_{\text{inv}}$  plane. Within the signal box, 19 events are found in the data while  $20.2 \pm 2.1$  events are expected from a background MC simulation and  $20.5 \pm 6.4$  events from the average  $M_{\text{inv}}$  sidebands. Figure 12 shows the  $\Delta E$  distribution of events with  $1.71 < M_{\text{inv}} < 1.82 \text{ GeV}/c^2$  (a signal region), which shows no excess over the expected background. An upper limit on  $Br(\tau \rightarrow \mu\gamma)$  is derived by fitting the background function to the  $\Delta E$  vs  $M_{\text{inv}}$  distribution of the data. Belle has obtained

$$Br(\tau \rightarrow \mu\gamma) < 3.1 \times 10^{-7}$$

at 90% C.L., which improves over the previous limits. It is evident that the improvement is limited by the remaining background in the signal region. Further rejection of the background is necessary to improve the sensitivity to contribution

from physics beyond the SM.

## 4 Conclusion

The presence of electroweak penguins has been established by  $B$ -factory experiments, Belle and BaBar. This opens up a new window to search for physics beyond the Standard Model. However, more data is clearly needed to detect a sign of new physics.

Similarly, the search for  $\tau \rightarrow \mu\gamma$  decay serves as a probe of new physics. Belle has obtained an improved upper limit on  $Br(\tau \rightarrow \mu\gamma)$  which helps to constrain possible scenarios for new physics. We wish to thank the organizers of SLAC Summer Institute for the great hospitality.

## References

- [1] For example, E. Lunghi *et al.*, Nucl. Phys. **B568**, 120 (2000); J.L. Hewett and J.D. Wells, Phys. Rev. D **55**, 5549 (1997); T. Goto *et al.*, Phys. Rev. D **55**, 4273 (1997); G. Burdman, Phys. Rev. D **52**, 6400 (1995); N.G. Deshpande, K. Panose, and J.Trampetic, Phys. Lett. B **308**, 322 (1993); W.S. Hou, R.S. Willey, and A.Soni, Phys. Rev. Lett. **58**, 1608 (1987).
- [2] R. Barbieri and L.J. Hall, Phys. Lett. B **338**, 212 (1994); J. Hisano *et al.*, Phys. Lett. B **357**, 579 (1995); J. Hisano and D. Nomura, Phys. Rev. D **59**, 116005 (1999); K.S. Babu, B. Dutta and R.N. Mohapatra, Phys.Lett. B **458**, 93 (1999); S.F. King and M. Oliveira, Phys. Rev. D **60**, 035003 (1999).
- [3] MARK-II Collaboration, K.G. Hayes *et al.*, Phys. Rev. D **25**, 2869 (1982).
- [4] ARGUS Collaboration, H. Albrecht *et al.*, Z. Phys. C **55**, 179 (1992).
- [5] DELPHI Collaboration, P. Abreu *et al.*, Phys. Lett. B **359**, 411 (1995).
- [6] CLEO Collaboration, A. Bean *et al.*, Phys. Re. Lett. **70**, 138 (1993), K.W.Edwards *et al.*, Phys. Rev. D **55**, R3919 (1997), S. Ahmed *et al.*, Phys. Rev. D **61**, 071101 (2000).
- [7] C. Brown (BaBar Collaboration), Nucl. Phys. B Proc. Suppl. **123**, 88 (2003).
- [8] Belle Collaboration, K. Abe *et al.*, Phys. Rev. Lett. **88**, 021801 (2002).
- [9] Belle Collaboration, J. Kaneko *et al.*, Phys. Rev. Lett. **90**, 021801 (2003).

- [10] Belle Collaboration, A. Ishikawa *et al.*, Phys. Rev. Lett. **91**, 261601 (2003).
- [11] BaBar Collaboration, B. Aubert *et al.*, Phys. Rev. Lett. **91**, 221802 (2003).
- [12] A. Ali, E. Lunghi, C. Greub and G. Hiller, Phys. Rev. D **66**, 034002 (2002).
- [13] BaBar Collaboration, B. Aubert *et al.*, hep-ex/0308016.
- [14] Belle Collaboration, K. Abe *et al.*, hep-ex/0310029.